Quantum chemistry with Coulomb Sturmians: Construction and convergence of Coulomb Sturmian basis sets at the Hartree-Fock level

Michael F. Herbst,[1,*] James Emil Avery,[2,†] and Andreas Dreuw[1,‡]

[1]*Interdisciplinary Center for Scientific Computing, Heidelberg University, Im Neuenheimer Feld 205, 69120 Heidelberg, Germany*
[2]*Niels Bohr Institute, University of Copenhagen, Blegdamsvej 17, 2100 København, Denmark*

A discussion of basis sets consisting of exponentially decaying Coulomb Sturmian functions for modeling electronic structures is presented. The proposed basis-set construction selects Coulomb Sturmian functions using separate upper limits to their principal, angular momentum, and magnetic quantum numbers. Their common Coulomb Sturmian exponent is taken as a fourth parameter. The convergence properties of such basis sets are investigated taking the second- and third-row atoms at the Hartree-Fock level as examples. Thereby, important relations between the values of the basis-set parameters and the physical properties of the electronic structure are recognized. Furthermore, a connection between the optimal, i.e., minimum-energy, Coulomb Sturmian exponent and the average Slater exponents values obtained by Clementi and Raimondi [J. Chem. Phys. **38**, 2686 (1963)] is made. These features of Coulomb Sturmian basis sets emphasize their ability to correctly reproduce the physical features of the Hartree-Fock wave functions. As an outlook, the application of Coulomb Sturmian discretizations for molecular calculations and post-Hartree-Fock methods is briefly discussed.

I. INTRODUCTION

The standard approach for approximating solutions to the electronic Schrödinger equation is to employ a limited set of single-particle basis functions to build a discretization basis. An early approach pursued by Slater [1] was to employ exponential-type orbitals (ETO) with a radial part of the form $\exp(-\zeta r)$ times a polynomial. In his construction the exponent ζ was estimated from empirical rules, but later refined exponents based on Hartree-Fock calculations became available [2]. Whilst ETO could thus be readily used for modeling atoms, difficulties related to the evaluation of multicentered two-electron repulsion integrals (ERI) directed attention to other types of basis functions for molecular calculations. An outcome of this development is contracted Gaussian-type orbitals (cGTO) [3,4], for which the evaluation of ERI is much simpler due to the Gaussian product theorem. Over the years, many kinds of cGTO basis sets have been developed [5,6], such that now most aspects of electronic structure can be modeled reliably using cGTO functions.

Compared to an ETO basis, a missing aspect of cGTO basis sets is, however, that these functions are not able to correctly reproduce the functional form [7,8] of the wave function at large distances or close to the nucleus. For properties such as nuclear-magnetic resonance (NMR) shielding tensors [9,10] or Rydberg-type or autoionizing states [11–14], where either the nuclear cusp or the asymptotic tail are important [9,10], ETO basis sets remain attractive. Additionally, the computational resources available for quantum-chemical calculations

have changed since the 1970's, such that it may now be favorable to invest extra computation per integral in order to have fewer, more accurate basis functions.

Following the pioneering efforts by Harris, Michels, Steinborn, Weniger, Weatherford, Jones, and others [15–18], in making ETOs more efficient, recently Coulomb Sturmians [19–24] (CS) have emerged as a particularly promising ETO basis. First, the momentum-space representation of these functions is equivalent to the hyperspherical harmonics, which allows multicenter electron repulsion integrals to be treated rather efficiently [25–28]. This opens the way for treating molecular problems based on these ETO in the future. Second, understanding CS basis sets provides a foundation towards the investigation of other ETO basis function types since the Coulomb Sturmian construction can be easily generalized preserving many useful properties of the CS functions [29]. For example, one may build N-particle basis functions that include geometric properties of the physical system under consideration at the level of the basis [29–37]. Similarly, d-dimensional hyperspherical harmonic basis sets can model collective motions of particles, for example, for treating strongly interacting few-body systems or reactive scattering [38–42]. With respect to scattering problems, employing Coulomb Sturmians and generalized Sturmians has become a well-established technique [43–48] and construction schemes for optimal Sturmian bases have been suggested [43].

In a recent publication we presented the MOLSTURM framework [49] in which atomic electronic-structure calculations based on a Coulomb Sturmian discretization can be performed both at Hartree-Fock (HF) and post-HF levels. Unlike the application of Sturmians to scattering and unlike conventional cGTO discretizations, construction schemes for reliable and efficient CS basis sets are not yet available to the best of our knowledge. The aim of this paper is to provide a first

*michael.herbst@iwr.uni-heidelberg.de
†avery@nbi.ku.dk
‡dreuw@uni-heidelberg.de

step towards closing this gap, allowing to readily conduct CS-based electronic-structure calculations in the future. In particular, this work is concerned with the construction of CS basis sets for atomic systems at the Hartree-Fock level, which represents a first elementary step for the construction of molecular basis sets. Appropriate modifications for capturing electronic correlation and to compute excited states will be briefly hinted at in the outlook. However, more detailed discussion on this matter is planned for a followup publication.

A. Coulomb Sturmian basis functions

Coulomb Sturmians are the analytic solutions to the single-particle equation [29]

$$\left(-\frac{1}{2}\Delta - \beta_n \frac{Z}{r} - E\right)\varphi_\mu^{\mathrm{CS}}(\underline{r}) = 0. \tag{1}$$

This equation can be considered as a modification of the hydrogenlike Schrödinger equation, where the Coulomb attraction between electron and nucleus is scaled by a factor

$$\beta_n = \frac{kn}{Z}. \tag{2}$$

Separation of (1) into radial and angular variables yields the *Coulomb Sturmian radial equation*

$$\left[-\frac{1}{2r^2}\frac{\partial}{\partial r}\left(r^2\frac{\partial}{\partial r}\right) + \frac{l(l+1)}{2r^2} - \frac{nk}{r} - E\right]R_{nl}(r) = 0. \tag{3}$$

Equation (3) defines the CS radial part R_{nl}, which is identical to the familiar hydrogenlike orbitals, just with all occurrences of the factors Z/r replaced by the Coulomb Sturmian exponent k. The full functional form of the CS reads as

$$\begin{aligned} \varphi_{nlm}(\underline{r}) &= R_{nl}(r)Y_l^m(\hat{\underline{r}}), \\ R_{nl}(r) &= k^{3/2}N_{nl}(2kr)^l e^{-kr}L_{n-l-1}^{2l+1}(2kr), \end{aligned} \tag{4}$$

where Y_l^m is a spherical harmonic, L_{n-l-1}^{2l+1} an associated Laguerre polynomial, and

$$N_{nl} = \frac{2}{(2l+1)!}\sqrt{\frac{(l+n)!}{n(n-l-1)!}} \tag{5}$$

the normalization constant. Next to other prominent atom-centered basis functions such as Slater-type orbitals (STO) or Gaussian-type orbitals, these functions share the factorization into a radial part R_{nl} and a spherical harmonic Y_l^m. In contrast to STO, however, all CS functions in a CS basis set share the exponent k, which furthermore is related to the energy eigenvalue of Eq. (1):

$$E = -\frac{k^2}{2}. \tag{6}$$

Similar to the Schrödinger equation for hydrogenlike atoms, Eq. (1) can only be solved for some quantum number triples (n, l, m), namely, those from the set

$$\mathcal{I}_F \equiv \{(n, l, m) \,|\, n, l, m \in \mathbb{Z} \quad \text{with}$$

$$n > 0,\ 0 \leqslant l < n,\ -l \leqslant m \leqslant l\}. \tag{7}$$

Furthermore, one follows the convention to call n, l, and m the principal, angular momentum, and magnetic quantum numbers and uses both the spectroscopic terminology $1s$, $2s$, $2p$, ... as well as the corresponding quantum number triple to refer to a particular CS function.

The Coulomb Sturmian radial equation (6) is of Sturm-Liouville form [21,29], equipping CS basis functions with some noteworthy properties. First, building on the arguments of Klahn and Bingel [50,51] one can show [52] the countably infinite set of all Coulomb Sturmians $\{\varphi_\mu^{\mathrm{CS}}\}_{\mu \in \mathcal{I}_F}$ to be a complete basis for the Sobelev space $H^1(\mathbb{R}^3)$ *independent* of the value of the exponent k. This is both the relevant Hilbert space for solving the one-particle Schrödinger equation [53] as well as the Hartree-Fock problem for many-body systems. As a consequence, the numerical challenges associated with treating high-energy Rydberg-type, dipole-bound, or ionizing states are most likely less pronounced with a CS-based approach.

Furthermore, the Sturm-Liouville form of the radial equation (3) implies that the radial parts R_{nl} form a complete basis for each value of l. We will employ this to design CS basis sets, which subsequently converge the radial part, but do not tighten the angular discretization beyond an initial level. Such basis-set progressions can be used to understand the maximal angular momentum quantum number required in a CS basis set for describing the wave function at a particular level of theory.

B. Importance of selecting angular momentum quantum numbers in quantum-chemical basis sets

Understanding which angular momentum quantum numbers are required in a basis is not a question limited to Coulomb Sturmians. Much rather this aspect is of general concern when constructing atom-centered basis sets for quantum-chemical modeling. In the familiar context of cGTO basis functions, for example, all basis sets used for practical calculations include at least polarization functions, i.e., functions whose angular momentum quantum number exceeds the minimal basis-set value. This allows both to capture the density reorganization going from atoms to molecular structures as well as the leading-order effects of electronic correlation [5,54–57]. Similarly, the systematic construction of cGTO basis sets with steady and reliable convergence behavior is closely related to selecting the amount of angular momentum to be included [58,59].

Additionally, investigating the required angular momentum quantum numbers can become a diagnostic tool. An example is the unphysical breaking of spherical symmetry in the unrestricted HF (UHF) modeling of atoms. When considering the results of an UHF calculation of carbon and fluorine, Cook [60] noticed the s-type and p-type HF orbitals for both these systems not to be linear combinations of cGTO basis functions with $l = 0$ and 1, but to involve functions with higher angular momentum quantum numbers as well. This was later found to be a general issue of UHF [61–63]. Reference [61] provides a detailed analysis of the underlying mechanisms including a discussion of the effect of symmetry breaking and HF instabilities in UHF and other HF variants.

Understanding which angular momentum quantum numbers a basis set needs to provide is thus of general importance to treat problems in molecular quantum chemistry and to understand their properties. With respect to Coulomb Sturmian discretizations, this work will discuss the root-mean-square occupied coefficient value per angular momentum (RMSO_l) to demonstrate the capabilities of such discretizations. As will be discussed, this quantity allows to directly observe the oddities with respect to the UHF-induced breaking of spherical symmetry. Furthermore, in general the angular momentum requirements of HF wave functions can be directly probed in this way. Similar to cGTO discretizations, our obtained results represent a step towards constructing more general CS basis sets for correlated methods or molecular calculations.

C. Paper outline

The remainder of the paper is structured as follows: Section II introduces the theoretical background and describes the computational methodologies. The obtained HF convergence results are discussed in Sec. III. Section IV provides an outlook towards post-HF methods and other directions of future work.

II. THEORY AND METHODOLOGY

A. Parameters for denoting Coulomb Sturmian basis sets

As outlined in Sec. I A, all Coulomb Sturmian functions share a common exponent k, but differ in the quantum numbers n, l, and m, which are taken from the set $\mathcal{I}_F$ [see Eq. (7)]. A Coulomb Sturmian basis set is therefore uniquely defined by denoting the selection of triples $(n, l, m) \in \mathcal{I}_F$ employed as well as the value for the exponent k.

Theoretically, any selection of triples $(n, l, m) \in \mathcal{I}_F$ can be used to form a CS basis. From the similarity of the CS functions to the hydrogenlike orbital functions, however, one can expect Coulomb Sturmians with smaller values of the principal quantum number n to be most important. Both chemical intuition as well as the typical construction schemes employed for cGTO basis sets [5] suggest to additionally limit the angular momentum quantum number l from above as well. Guided by these ideas, we focus in our investigation on CS basis sets of the form

$$\mathcal{I}_{\text{bas}} \equiv \big\{ \varphi_{nlm} \,|\, (n, l, m) \in \mathcal{I}_F, \; n \leqslant n_{\max}, \; l \leqslant l_{\max},$$
$$-m_{\max} \leqslant m \leqslant m_{\max} \big\}, \tag{8}$$

i.e., where all three quantum numbers are bound from above. For ease of notation, we will refer to CS basis sets like Eq. (8) by the triple $(n_{\max}, l_{\max}, m_{\max})$. For example, a (3,2,2) CS basis denotes the set with $n_{\max} = 3$, $l_{\max} = 2$, and $m_{\max} = 2$. Typically, we will not place explicit bounds on all three quantum numbers. For example, m is usually not restricted beyond the limit $|m| < l$ intrinsic to the CS equation (1). We will refer to such a basis as being only restricted by $n_{\max}$ and $l_{\max}$. Similarly, a basis only restricted by $n_{\max}$ has no tighter bound on l apart from the condition $l < n$ already encoded in $\mathcal{I}_F$.

Tuning the maximal quantum numbers $n_{\max}$, $l_{\max}$ and $m_{\max}$ naturally influences the subset of radial functions R_{nl} and spherical harmonics Y_l^m, which is available in the discretization basis. Since the Coulomb Sturmian radial equation (3) is of Sturm-Liouville form, the eigenfunctions of Eq. (3), i.e., the set of all radial functions $\{R_{nl'}\}_{n>0}$ with l' fixed, is a complete basis for a weighted L^2 space [52]. This allows to express each function R_{nl} with arbitrary l as a linear combination of functions $\{R_{n',l'}\}_{n'>0}$ of a different l'. By considering the polynomial spaces spanned by the CS radial functions, one can show that for given n and l a set consisting only of the radial parts with $l' = 0$ and $n' \leqslant n$ is sufficient to form R_{nl}. As a result,

$$\forall\, n_{\max} > 0, 0 \leqslant l < n_{\max} : \; \text{span}\{R_{n'l'}\}_{n' \leqslant n_{\max}, l' \leqslant l}$$
$$= \text{span}\{R_{n',0}\}_{n' \leqslant n_{\max}}. \tag{9}$$

Convergence in the radial discretisztion in a CS basis can thus be completely controlled by tuning the bound $n_{\max}$. Conversely, $l_{\max}$ and $m_{\max}$ only effect convergence with respect to the angular part in agreement with the physical interpretation given to the quantum numbers l and m. Notice that these arguments are independent of the value of k, and as such apply for any value of the CS exponent.

Provided that a value for $l_{\max}$ has been found, which provides a good enough angular discretization, additional convergence in the radial coordinates can therefore be achieved by only increasing the bound $n_{\max}$ of the CS basis. The implied strategy, namely, to restrict both $n_{\max}$ and $l_{\max}$, possesses the additional advantage that the scaling of the basis size with respect to $n_{\max}$ is reduced compared to only restricting $n_{\max}$. Explicitly, in the latter case the resulting basis consists of

$$N_{\text{bas}}(n_{\max}) = \sum_{n=1}^{n_{\max}} \sum_{l=0}^{n-1} \sum_{m=-l}^{l} 1 = \sum_{n=1}^{n_{\max}} \sum_{l=0}^{n-1} 2l + 1$$
$$= \sum_{n=1}^{n_{\max}} n^2 = \frac{(2n_{\max} + 1)(n_{\max} + 1)n_{\max}}{6}$$
$$\in O(n_{\max}^3) \tag{10}$$

functions, i.e., scales cubically with $n_{\max}$. In comparison, an additional restriction by $l_{\max}$ leads to

$$N_{\text{bas}}(n_{\max}) = \sum_{n=1}^{n_{\max}} \sum_{l=0}^{\min(l_{\max}, n-1)} 2l + 1$$
$$= \sum_{n=1}^{n_{\max}} (\min(l_{\max} + 1, n))^2$$
$$\leqslant \sum_{n=1}^{n_{\max}} (l_{\max} + 1)^2 = (n_{\max} - 1)(l_{\max} + 1)^2$$
$$\in O(n_{\max} l_{\max}^2), \tag{11}$$

i.e., linear scaling in $n_{\max}$. Since the prefactor depends on $l_{\max}^2$, however, a small value for $l_{\max}$ is desirable.

B. Hartree-Fock variants and fractional occupation scheme

All variants of Hartree-Fock (HF) [64–66] can be viewed as a minimization procedure of an appropriate energy functional with respect to the occupied HF or density functional

theory (DFT) orbitals [67–69]. Employing a finite-sized basis set for the discretization and separating the resulting Euler-Lagrange equations into α and β spin components yields the following system of coupled nonlinear eigenvalue problems:

$$\mathbf{F}^{\sigma}(\mathbf{D}^{\alpha}, \mathbf{D}^{\beta})\mathbf{C}^{\sigma} = \mathbf{S}\mathbf{C}^{\sigma}\mathbf{E}^{\sigma},$$

$$\mathbf{C}^{\sigma\dagger}\mathbf{S}\mathbf{C}^{\sigma} = \mathbf{I}, \tag{12}$$

where $\sigma \in \{\alpha, \beta\}$ indicates the spin component, $\mathbf{C}^{\sigma}$ are the matrices of orbital coefficients, $\mathbf{E}^{\sigma}$ the diagonal matrices of orbital energies, $\mathbf{S}$ is the overlap matrix, and $\mathbf{I}$ the identity matrix. The nonlinearity of (12) originates from the Fock matrix since $\mathbf{F}(\mathbf{D}^{\alpha}, \mathbf{D}^{\beta})$ depends on both densities $\mathbf{D}^{\sigma}$. These in turn are related to the coefficients $\mathbf{C}^{\sigma}$ via

$$\mathbf{D}^{\sigma} = \mathbf{C}^{\sigma}\mathbf{f}^{\sigma}\mathbf{C}^{\sigma\dagger}, \tag{13}$$

where $\mathbf{f}^{\sigma}$ is the diagonal matrix of occupation numbers. Equations (12) may be solved iteratively employing the *self-consistent field procedure* (SCF) [64]. For restricted closed-shell HF (RHF) [64] one takes $\mathbf{F}^{\alpha} = \mathbf{F}^{\beta}$, which implies $\mathbf{D}^{\alpha} = \mathbf{D}^{\beta}$. Thus, Eq. (12) only needs to be solved for one component, say for $\sigma = \alpha$. For unrestricted HF, on the other hand, this restriction is not applied [65] and both components may diverge during an SCF.

The spin component restriction of RHF implies that only closed-shell atomic systems can be treated. For open-shell atoms, typically UHF is employed instead. As already discussed in Sec. I B, an UHF treatment of open-shell atoms, however, typically suffers from issues related to a breaking of spherical symmetry.

To illustrate this, consider the carbon atom with its ninefold-degenerate ^{3}P ground state. Not considering the spin degeneracy, three energetically equivalent ground-state Slater determinants exist, which differ only in projected angular momentum L_z. In a full configuration interaction treatment, spherical symmetry could therefore be recovered forming the ground-state wave function from a linear combination of these determinants. For UHF this is not possible due to the single-determinant nature of HF. As a result, the UHF density matrix is symmetry broken and the SCF procedure yields orbitals that are no longer of pure s, p, d, ... character. Such issues are naturally not restricted to ground states with a P term, but will occur similarly for all atoms with a ground state of total angular momentum $L > 1$.

An additional approximation to circumvent this behavior is to employ *fractional occupation numbers* (FON). This approach emerged from developments to reproduce the spectra of radical hydrocarbon species [70–74], where the so-called *half-electron method* [75] was suggested as a simpler alternative to the restricted open-shell [76] procedure. In the context of UHF, the FON approach distributes the valence electrons evenly over those valence orbitals differing only in the magnetic quantum number. For the open-shell atoms of the second and third periods considered in this work, this implies that an equal electron population in the $2p$ or $3p$ orbitals is achieved by selecting fractional values between 0 and 1 for those entries of the occupation matrix $\mathbf{f}^{\sigma}$ corresponding to said orbitals. This effectively allows the UHF procedure to converge to a determinant, which is an average over those

$2L + 1$ degenerate determinants one would actually need to combine in order to recover spherical symmetry.

It should be noted, however, that a fractional occupation is no longer in accordance with the Aufbau principle, where the entries of $\mathbf{f}$ would be either 1, namely, for all occupied orbitals, or 0, for all virtual orbitals. This implies (1) that the resulting HF density matrices are no longer idempotent and (2) that the obtained solution of Eq. (12) cannot be a stationary point of the HF minimization problem [77]. In other words, the FON approach represents an additional approximation on top of UHF and the obtained energies will be *higher* compared to integer occupation. As outlined in Ref. [71] with respect to the half-electron methods, however, the difference between the integer and fractional approaches can be expected to be small, such that for many practical calculations both methods are typically similarly suitable.

C. Probing the required maximal angular momentum in HF calculations

Summarizing the discussion in Sec. II A, it is clear that choosing a suitable, but small value for $l_{\max}$ to reach the desired level of accuracy is important for CS-based discretizations, too. Similarly, understanding the angular momentum quantum numbers required in a discretization basis can help to understand the properties of quantum-chemical methods.

From an intuitive point of view, one would not expect all angular momentum to be equally important for the description of the electronic ground state of a particular atom. In beryllium, for example, only the $1s$ and $2s$ atomic orbitals are occupied, such that only angular momentum $l = 0$ seems to be required. Conversely, all CS functions with $l > 0$ should contribute only very little, if at all. Guided by this hypothesis, the *root-mean-square occupied coefficient* per angular momentum l (RMSO$_l$) is defined as

$$\mathrm{RMSO}_l = \sqrt{\sum_{(n,l,m) \in \mathcal{I}_{\mathrm{bas}}} \sum_{i} \sum_{\sigma \in \{\alpha, \beta\}} \frac{1}{N_{\mathrm{elec}}^{\sigma} N_{\mathrm{bas},l}} \left(C_{\mu,i}^{\sigma} f_{ii}^{\sigma}\right)^2}, \tag{14}$$

where i runs over all SCF orbitals, $\mathcal{I}_{\mathrm{bas}} \subset \mathcal{I}_{F}$ is the selected set of index triples $\mu \equiv (n,l,m)$ for the CS basis functions, and $N_{\mathrm{elec}}^{\sigma}$ are the number of electrons of spin σ. Furthermore, $C_{\mu i}^{\alpha}$, $C_{\mu i}^{\beta}$, f_{ii}^{α}, and f_{ii}^{β} are the matrix elements of the orbital coefficient matrices and occupation matrices introduced in Sec. II B and

$$N_{\mathrm{bas},l} := \left| \left\{ (n',l',m') \,\middle|\, (n',l',m') \in \mathcal{I}_{\mathrm{bas}} \text{ and } l' = l \right\} \right| \tag{15}$$

is the number of basis functions in the CS basis which have angular momentum quantum number l. By construction, RMSO$_l$ is the root-mean-square (RMS) coefficient for a particular angular momentum quantum number l in the occupied SCF orbitals. It therefore provides a measure, which angular momentum quantum numbers l of the current basis set are used in a significant amount for describing the HF wave function, namely, those where RMSO$_l$ is above the convergence threshold of the SCF procedure.

To use this quantity for finding a good value of $l_{\max}$ to restrict the CS basis first a HF calculation is performed, where

the employed CS basis set is only restricted by n_{max}. This value n_{max} should be chosen carefully since on the one hand too large a value leads to rather large basis sets and thus potentially expensive calculations and on the other hand too small a value implies that l does not reach large enough values to observe a visible trend. In this work we used a (6,5,5) basis set for this step. Afterwards, an RMSO$_l$ plot, i.e., plot RMSO$_l$ versus l, is produced and the trends observed. Since larger l implies more angular nodes thus higher kinetic energy, larger values of l will become less and less significant, i.e., RMSO$_l$ will decrease. Inspecting the plot an l_{max} can then be chosen such that those angular momentum quantum numbers larger l_{max} can be considered insignificant. See Sec. III A for examples.

In analogy to Eq. (14) we can furthermore compute a root-mean-square coefficient value per basis function angular momentum quantum number l for each SCF orbital. This quantity will be used in Sec. III A to explain the behavior of RMSO$_l$ plots.

D. Computational details and reference values

All HF computations presented in this work were obtained using the STURMINT [78] Coulomb Sturmian integral library in combination with the MOLSTURM framework [49] or the SELF-CONSISTENTFIELD.JL [79] code to drive the SCF computation. Postprocessing and plotting was done in PYTHON [80] and JULIA [81] using MOLSTURM, NUMPY [82,83], PANDAS [84], and MATPLOTLIB [85].

RHF was employed to compute the energies of closed-shell atoms, whereas UHF was used for open-shell systems. If not explicitly mentioned otherwise, the UHF results refer to calculations employing integer occupation numbers. For carbon and oxygen some UHF calculations with fractional occupation were underdone as well, where an occupation of $\frac{2}{3}$ was used for the $2p\alpha$ orbitals of carbon and of $\frac{1}{3}$ for the $2p\beta$ orbitals of oxygen. The estimation of errors and convergence was done by comparing our CS-based HF results with the reference values of Table I. These include, for RHF calculations, the numerical RHF energies obtained by Morgon *et al.* [87]. For UHF calculations, the complete basis set (CBS) limit was extrapolated following the approach of Jensen [91] applied to calculations with the Dunning cc-pVnZ family of cGTO basis sets [58,86,88–90].

III. RESULTS AND DISCUSSION

This section presents the results of our convergence study of CS basis sets for discretizing the HF problem, obtained for the atoms of the second and third periods of the periodic table. We expect the outlined procedures to be of general character, however, such that they could be applied to the remainder of the periodic table as well.

A. Convergence with respect to basis set size and angular momentum analysis

As described in Sec. II A the construction of Coulomb Sturmian basis sets consists of the selection of roughly two types of parameters. First, n_{max} and l_{max}, which fix the size

TABLE I. Reference values used for comparison of the CS-based results and for estimating errors in the CS values. The CBS extrapolation was done following Jensen [91]. Superscript U denotes unrestricted HF with integer occupation numbers; superscript F denotes unrestricted HF with fractional occupation numbers; and superscript R denotes restricted HF.

System	E_{HF}	System	E_{HF}
Li	$-7.4327376^{U,a}$	Na	$-161.8589459^{U,a}$
Be	$-14.57302317^{R,b}$	Mg	$-199.61463642^{R,b}$
B	$-24.5334831^{U,a}$	Al	$-241.8808503^{U,c}$
C	$-37.6937751^{U,c}$	Si	$-288.8589476^{U,c}$
C	$-37.5313456^{F,c}$		
N	$-54.4046409^{U,c}$	P	$-340.7192829^{U,c}$
O	$-74.8192096^{U,c}$	S	$-397.5133666^{U,c}$
O	$-74.624862^{F,c}$		
F	$-99.4166858^{U,c}$	Cl	$-459.4899302^{U,c}$
Ne	$-128.54709811^{R,b}$	Ar	$-526.8175128^{R,b}$

^aCBS extrapolation using cc-pVDZ to cc-pV5Z [58,86].
^bValues taken from Morgon *et al.* [87].
^cCBS extrapolation using cc-pVTZ to cc-pV6Z [58,86,88–90].

of the basis and second, k, which communally fixes the exponential falloff of all basis functions.

In this section we will primarily discuss convergence with respect to the first aspect, i.e., the CS basis-set size. As outlined in the previous sections, both the completeness of the CS radial part R_{nl} as well as the CS functions φ_{nlm} is independent of the exponent k. The general convergence trend with respect to increasing basis-set size can thus be expected to be independent of the value of k as well. There is, however, a notable effect on the convergence rate with increasing basis size. This is demonstrated in Fig. 1, which shows the convergence of the HF energies of beryllium and
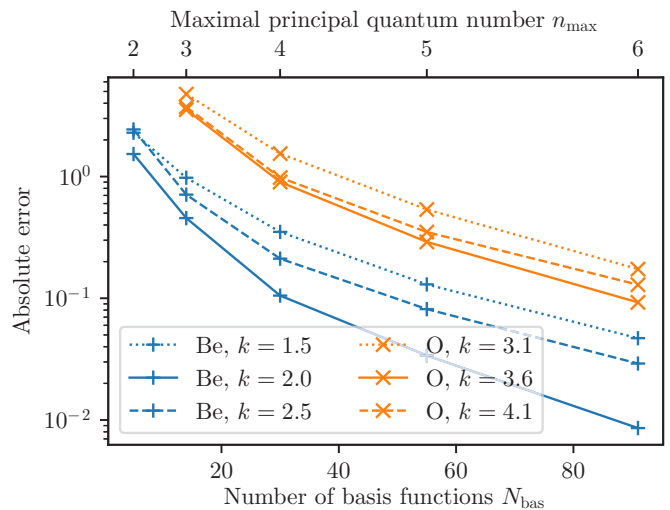

FIG. 1. Absolute error in the HF energy versus number of basis functions in a CS basis set only restricted by the maximal principal quantum number n_{max} (top axis). The blue curves are RHF calculations of beryllium, the orange curves UHF calculations of oxygen, each with different CS exponents k. The reference values for the error computation were taken from Table I.
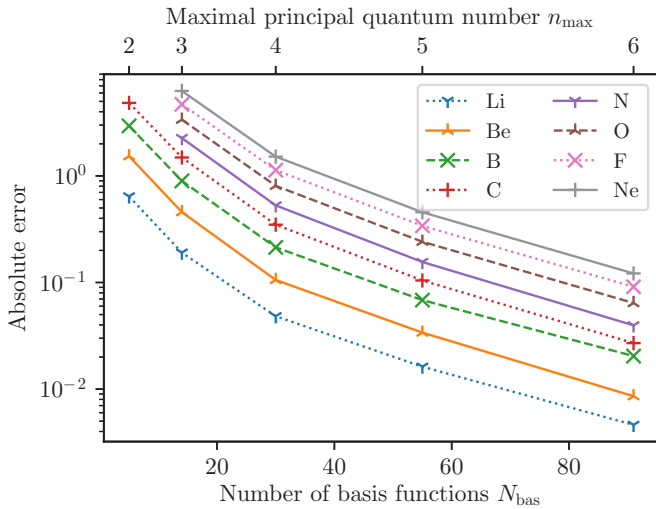
FIG. 2. Plot of the absolute error in the HF energy versus the number of basis functions in a CS basis restricted by n_{max}. For the closed-shell atoms Be and Ne, the restricted HF procedure was used, whereas for the other systems UHF with integer occupation was employed. For each calculation of a particular atom the same value of k was used, which was taken within 0.01 to the optimal exponent of this atom at (6,5,5) level. The errors were computed against the reference values from Table I.

oxygen, respectively. In both cases, the absolute error versus the reference values (see Table I) is plotted against the size of the employed CS basis sets, which are only restricted by the indicated maximal principal quantum number n_{max}. As expected by the Courant-Fischer variational theorem [92], a decrease in error can be observed for larger basis sets, i.e., larger values for n_{max}. For all curves the convergence appears to be sublinear with the best rate of convergence achieved for $k = 2.0$ for beryllium and $k = 3.6$ for oxygen. Larger as well as smaller exponents worsen the convergence rate, which will be discussed in more detail in Sec. III B. For the discussion in this section it is sufficient to note that convergence is achieved regardless of the value of k, but some optimal, atom-dependent value exists for each CS basis set, where the HF energy is lowest.

Such observations are in agreement with previous results obtained by Avery and Avery [28], where they approximated Slater-type orbitals (STO) in a basis of Coulomb Sturmians. In their treatment they also found that convergence is faster the closer the CS exponent of the basis to the STO exponent of the function to be approximated, but convergence occurred in either case. For understanding the convergence behavior with respect to increasing the basis-set size, the dependency on k can thus be largely ignored, provided that for each atom a reasonable value for k is chosen.

The convergence trend observed in Fig. 1 for beryllium and oxygen appears to be more general. Our investigations show that it can at least be replicated in a similar fashion for the other atoms of the second period (see Fig. 2) as well as the third period. In all these calculations, the convergence is noticeably sublinear and overall comparatively slow. Already for the second half of the second period reaching below absolute errors of 0.1 hartree requires beyond 80 basis functions,
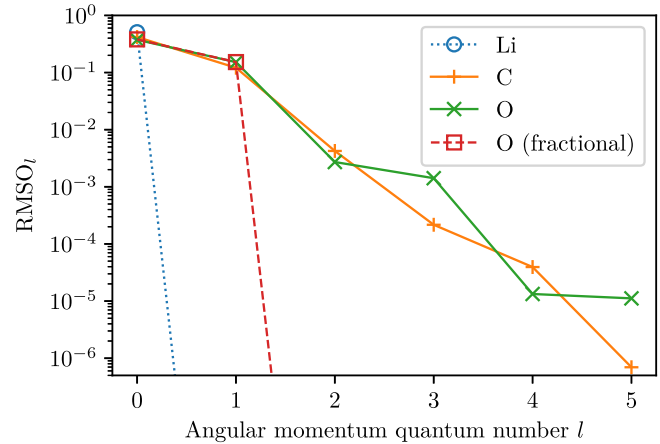

FIG. 3. Plot $RMSO_l$ vs l for the UHF ground state of the atoms of the second period if a (6,5,5) CS basis is employed. In each case, k was taken within 0.01 to the optimal exponent. For oxygen, both a case with integer and a case with fractional occupation numbers are depicted.

making calculations with Coulomb Sturmian basis sets only restricted by n_{max} rather impractical.

In Sec. II A we deduced that the basis size scaling with respect to n_{max} can be reduced from cubic to linear if the basis can be restricted by l_{max} as well, which evidently has an impact on the convergence speed. In order to find bounds for l_{max}, the $RMSO_l$ measure introduced in Sec. II C is applied to the SCF coefficients obtained in a (6,5,5) CS basis. For the UHF calculations of lithium, carbon, and oxygen, plots of $RMSO_l$ vs l are shown in Fig. 3. Corresponding plots for the other atoms of the second and third periods can be found in Figs. 4 and 5.

In all aforementioned plots, roughly two trends can be identified. The first is a very pronounced drop in $RMSO_l$, which occurs once a particular angular momentum value l

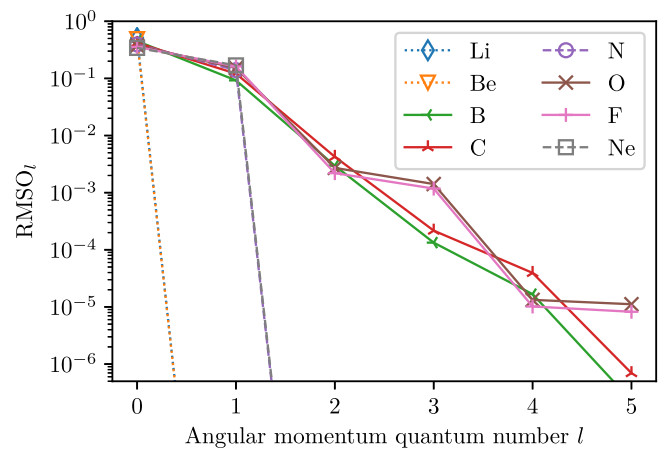FIG. 4. Plot $RMSO_l$ vs l for the HF ground state of the atoms of the second period if a (6,5,5) CS basis is employed. In each case, k was taken within 0.01 to the optimal exponent. For Be and Ne, a RHF procedure was used, for the other cases UHF with integer occupation numbers. The graphs for Li and Be as well as N and Ne with their respective sharp drop features are almost superimposed.
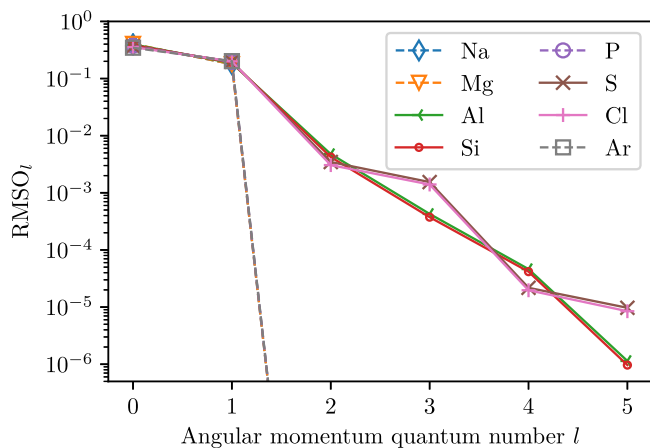
FIG. 5. Plot RMSO$_l$ vs l for the HF ground state of the atoms of the third period if a (6,5,5) CS basis is employed. In each case, k was taken close to the optimal value. For Mg and Ar, a RHF procedure was used, for the other cases UHF with integer occupation numbers. The graphs for Na, Mg, P, and Ar are almost superimposed.

has been reached. For example, in Fig. 3 this is observed for lithium (between $l = 0$ and 1) and oxygen with fractional occupation numbers (between $l = 1$ and 2). The second is a decreasing staircase pattern, where the RMSO$_l$ value decreases only very moderately over the range of considered angular momentum quantum numbers. In Fig. 3, for example, this is observed for oxygen with integer occupation numbers as well as for carbon. Considering the atoms of the second and the third periods altogether, the rapid-drop-type RMSO$_l$ plots are obtained for those atoms with an S ground-state term. That is, those which are either closed shell like Be, Ne, Mg, or Ar or which have a half-filled s or p shell like Li, N, Na, or P. In these cases, the drop occurs exactly where one would expect by looking at the largest angular momentum of the occupied atomic orbitals, i.e., between $l = 0$ and 1 for Li and Be, and between $l = 1$ and 2 for the other mentioned cases. In contrast to this, the atoms with a P ground-state term, namely, B, C, O, F, Al, Si, S, and Cl, follow the decreasing staircase pattern, but only if fractional occupation numbers are not used.

A hint to explain the second type of behavior is obtained by looking at the RMS coefficient values per basis function angular momentum quantum number l for each orbital (for details see Sec. II C). A plot of these values against l is shown in Fig. 6 for oxygen. Surprisingly, the 2s UHF orbital not only consists of basis functions with $l = 0$, but furthermore of functions with $l = 2$ and 4 in the employed (6,5,5) CS basis. Similar observations can be made for the 2p and 3d functions, which are not angular momentum pure any longer, but consist of angular momentum in steps of 2 apart. This behavior explains why RMSO$_l$ plots for oxygen do not show the expected drop from $l = 1$ to 2 since the higher angular momenta play a role for the occupied s-type and p-type SCF orbitals as well. This observed behavior is in perfect agreement with the breaking of spherical symmetry previously observed in UHF calculations [60–63]. As described in Ref. [63] the UHF wave function in such cases is not spherically, but *axially* symmetric. On the level of the SCF orbitals themselves, this is realized by mixing with higher
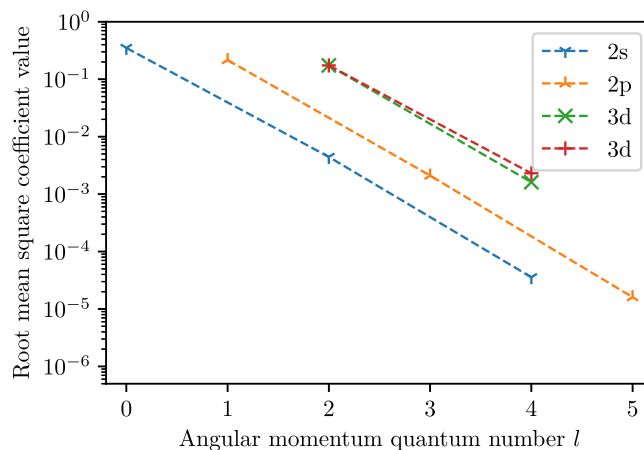

FIG. 6. Root-mean-square coefficient value per basis function angular momentum quantum number l for selected orbitals of oxygen. The atom is modeled in a (6,5,5) CS basis using UHF.

angular momentum basis functions. For illustration, consider amending a spherically symmetric s orbital with a fraction of a d_{z^2} basis function d_{z^2}. This causes a stretching of the orbital along the z axis, which makes it axially symmetric. Similarly, the p_x, p_y, and p_z orbitals may be amended with f_{xz^2}, f_{yz^2}, and f_{z^3} to elongate them in the z direction. Since parity may not be violated, an orbital may only consist of basis functions with either even or with odd angular momentum, explaining the pattern of Fig. 6, where either the even or the odd values are missing. For other calculations, which show the decreasing staircase RMSO$_l$ pattern, similar plots to Fig. 6 with smeared-out angular momentum are obtained. See, for example, carbon in Fig. 7. Conversely, if the SCF orbitals are pure in angular momentum, a clear drop in the RMSO$_l$ plots is observed. One example is nitrogen (Fig. 8) or oxygen at UHF level with fractional occupations. This confirms our discussion in Sec. II B indicating that an S ground-state term or an UHF treatment with fractional occupation numbers prevents a breaking of spherical symmetry.
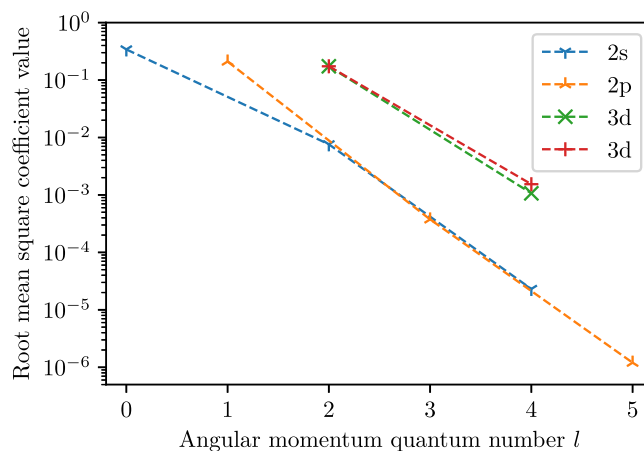

FIG. 7. Root-mean-square coefficient value per basis function angular momentum quantum number l for selected orbitals of carbon. The atom is modeled in a (6,5,5) CS basis using UHF.
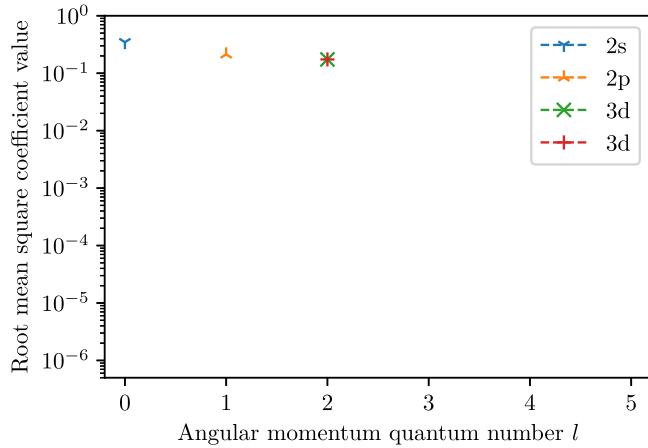
FIG. 8. Root-mean-square coefficient value per basis function angular momentum quantum number l for selected orbitals of nitrogen. The atom is modeled in a (6,5,5) CS basis using UHF.

With this in mind, a bound for l_{max} is easy to choose for those $RMSO_l$ plots with a clearly observable drop, namely, exactly the value for the angular momentum quantum number l *before* the drop is encountered. For the cases with a decreasing staircase pattern, the selection is not so straightforward since l_{max} both influences the prefactor in the scaling of basis size versus n_{max} [see Eq. (11)] as well as the angular discretization a basis provides. To observe the influence of different choices for n_{max} and l_{max}, Fig. 9 shows RHF or UHF results obtained using progressions of CS basis sets, where l_{max} is limited to either 0, 1, or 2, but n_{max} is ranged between 4 and 12. In each case, the relative error of the HF energy with respect to the reference values in Table I is plotted against the size of the CS basis. Those error values corresponding
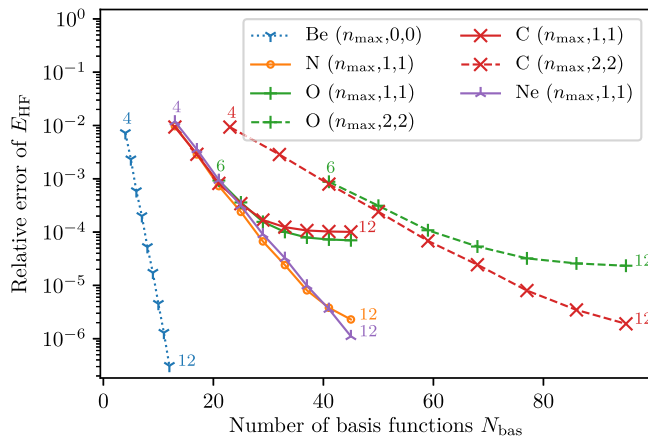

FIG. 9. Relative error in E_{HF} versus the number of basis functions for selected CS basis sets of the form $(n_{max}, l_{max}, l_{max})$. The connected points show basis-set progressions in which the maximum principal quantum number n_{max} is increased in steps, while l_{max} is kept fixed. The first and last values for n_{max} are denoted as small numbers next to appropriate data points. The same line type is used for all progressions of the same l_{max} and the same color and marker for all progressions of the same atom. For Be and Ne, RHF was used and for N, C, and O UHF.
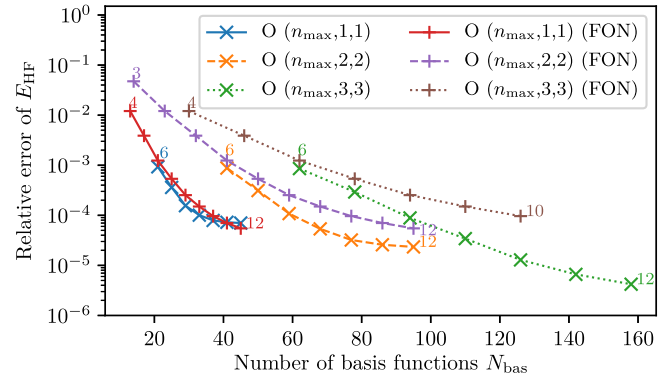

FIG. 10. Relative error in E_{HF} versus the number of basis functions for selected basis-set progressions. Shown are UHF calculations of oxygen using either integer or fractional occupation numbers (FON). The same display conventions as Fig. 9 are used.

to the same atom and the same l_{max}, but different n_{max}, are connected by lines. In the following, we will refer to such a sequence of calculations, in which only n_{max} differs by the term *progression*. In all calculations, for a particular atom the CS exponent k has been kept constant.

In agreement with the conclusions from the $RMSO_l$ plots, a very good convergence with respect to increasing n_{max} is observed for beryllium, nitrogen, and neon even if the angular momentum is restricted by $l_{max} = 0$ or $l_{max} = 1$. A further increase of l_{max} does not improve the obtained error regardless of the value of n_{max}. Since the basis now grows faster as n_{max} increases, the convergence rate is slower in such cases, however. This is in contrast to oxygen and carbon. As the $RMSO_l$ plots in Fig. 3 suggest, the angular momentum values $l > 2$ are required for a proper description of the symmetry-broken UHF ground state. It is therefore no surprise that the convergence of the HF energy begins to stagnate for the n_{max} progressions with $l_{max} = 1$ as well as $l_{max} = 2$. In these cases, a relevant part of the ground-state wave function cannot be represented in the available angular discretization and at some point the resulting error in the angular discretization dominates. Improving the radial discretization by increasing n_{max} thus cannot decrease the net error any further. The obtained limiting relative error depends on l_{max}, with larger values of l_{max} allowing a basis progression to yield a lower error limit. The obtained limits are further system dependent and their trends with l_{max} can be understood looking at the decreasing staircase patterns. For example, the limiting error in the $l_{max} = 1$ and 2 progressions for oxygen is almost unchanged, whereas it is significantly smaller for carbon. At the same time, considering the $RMSO_l$ plots in Fig. 3, the decrease in the $RMSO_l$ value from $l = 1$ to 2 is small for O, but a good order of magnitude for the C atom. Going to larger angular momentum, the $RMSO_l$ plot for oxygen with integer occupation undergoes a significant decrease between $l = 2$ and 3, however. In agreement the limiting error of a oxygen $l_{max} = 3$ progression decreases as well (see Fig. 10), which shows the $l_{max} = 1$, 2, and 3 progressions for oxygen with both integer and fractional occupations. As discussed in Sec. II B, fractional occupation numbers prevent symmetry breaking, such that pure angular momentum SCF orbitals are
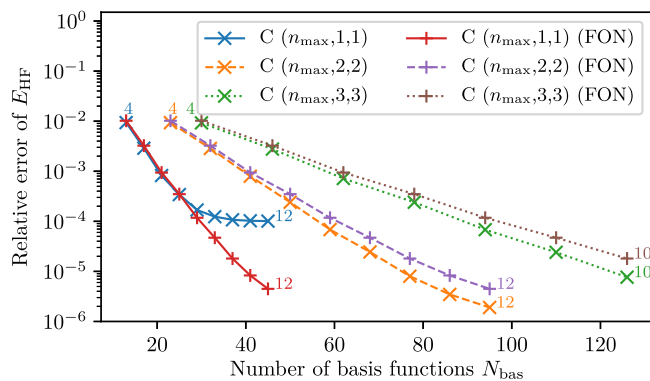
FIG. 11. Relative error in E_{HF} versus the number of basis functions for selected basis-set progressions. Shown are UHF calculations of carbon using either integer or fractional occupation numbers (FON). The same display conventions as Fig. 9 are used.

FIG. 12. Plot of the HF energy contributions of the carbon atom versus the Coulomb Sturmian exponent k. All calculations are done in a (5,2,2) CS basis using UHF.

obtained. As a consequence, only pure s and p functions are occupied and no improvement in UHF energies is obtained for the progressions with $l_{max} > 1$. For comparison, an equivalent plot to Fig. 10 for carbon is shown in Fig. 11.

An interesting aspect to note in all plots of relative error versus basis-set size is the initial convergence, which seems to follow a linear behavior in all depicted cases. Furthermore, the initial rate appears to depend only on l_{max}, but notably not on the system under investigation. As the progression continues, most curves bent off to become sublinear. A closer inspection, however, reveals two kinds of trends, which are best visible for the $l_{max} = 1$ progressions in Fig. 10 as well as Fig. 11. For the integer occupation numbers, the previously discussed stagnation of convergence is observed, which we could explain with reference to the decreasing staircase pattern in the $RMSO_l$ plots and too small a value for l_{max}. For the fractional occupation numbers, the curves do not not completely stagnate, but merely slow down. This is also observed for some other cases, e.g., N in Fig. 9, where the $RMSO_l$ plot allows to point out a particular value l_{max}, where all angular discretization of the HF wave function should be obtained. Such sublinear convergence behavior is not an unusual result in electronic structure theory. See, for example, Ref. [91] for a discussion of CBS extrapolations using cGTO basis sets or Ref. [93] for error estimates for even-tempered Gaussian-type basis sets. In combination with the apparently system-independent initial convergence, this indicates that rigorous CBS extrapolation techniques are within reach for CS basis sets as well.

B. Convergence with respect to the Coulomb Sturmian exponent k

Having discussed convergence with CS basis-set size in the previous sections, we now turn our attention to the CS exponent k. In Fig. 1 of Sec. III A, we already noted the convergence rate of CS discretizations to depend on k with some values giving faster and some slower convergence. For constructing a basis, which approximates the wave function best given a particular CS basis size, a suitable exponent k needs to be chosen as well. This section will discuss the influence of altering the CS exponent k in more detail.
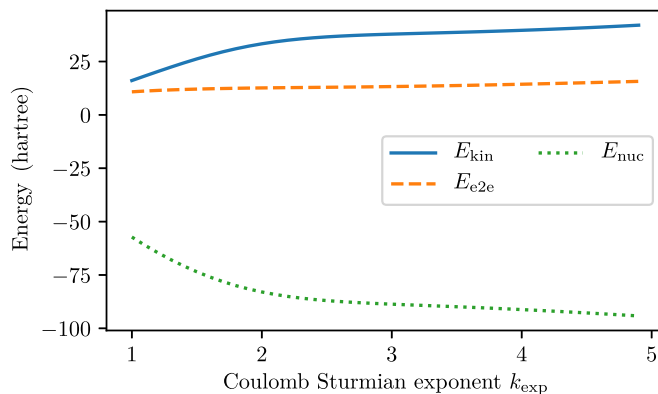
In the CS basis functions, k only occurs in the radial part [see Eq. (4)]. Through the exponential term $\exp(-kr)$, k influences how quickly the basis functions decay asymptotically and in the form of a polynomial prefactor it determines the curvature of the radial functions as they oscillate between the radial nodes. Keeping this in mind, let us consider Fig. 12, which shows the changes to individual energy contributions of the HF ground-state energy as k is altered. The largest changes are apparent for the nuclear attraction energy (E_{nuc}), which decreases, initially rather steeply, as k is increased. This can be easily understood from a physical point of view. Since larger values of k imply a more rapid decay of the basis functions, the electron density on average stays closer to the nucleus, which in turn leads to a lower (more negative) interaction energy between electrons and nucleus. The converse effect happens for smaller values of k, where the electron density is more expanded and thus on average at larger distance from the nucleus. In contrast, the kinetic energy (E_{kin}) is related to the curvature of the wave function, which, as described above, increases for larger k. In other words, the trends of nuclear attraction energy and electronic kinetic energy oppose each other, with the kinetic energy being affected to a lesser degree. On the scale depicted in Fig. 12, the variation of the electron-electron interaction (E_{e2e}), i.e., both classical Coulomb repulsion as well as the exchange interaction combined, is much less pronounced. Only a very minor increase with k can be observed. The physical mechanism is again similar to the nuclear attraction energy term, namely, that larger k compresses the wave function and thus lets the electrons reside more closely to another, which increases the Coulomb repulsion between them. The exchange interaction is affected as well, but changes are smaller and thus hidden in the trend of the Coulomb term. Notice that the observed opposing trends of the two largest depicted terms, the kinetic and nuclear attraction energies, are in agreement with the virial theorem. Since this requires the sum of the potential energy terms ($E_{nuc} + E_{e2e}$) to be related to the kinetic energy by a factor of -2, the same should hold true for the slopes of these as k is varied. Neglecting the electron-electron interaction, this relationship can indeed be roughly observed for the two other curves.

Summing up, all energy contributions lead to curves such as Fig. 13, which shows the total Hartree-Fock energy versus
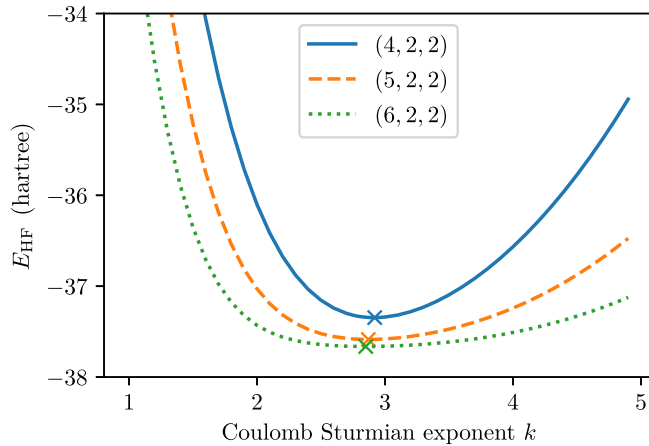
FIG. 13. Plot of the UHF energies of carbon versus the Coulomb Sturmian exponent k in the $(4,2,2)$, $(5,2,2)$, and $(6,2,2)$ basis sets. The minimum-energy exponent k_{opt} for each basis set is marked by a cross.
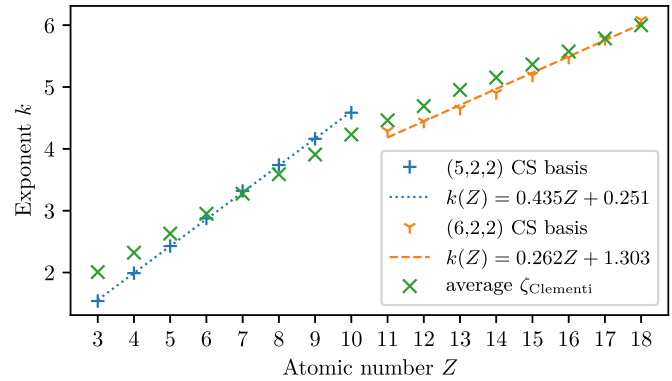

FIG. 14. Plot of the atomic number versus the optimal Coulomb Sturmian exponent k_{opt} for the atoms of the second and the third periods. For comparison, the occupation-averaged value of the Clementi and Raimondi [2] optimal Slater exponent $\zeta_{Clementi}$ is shown as well.

the Coulomb Sturmian exponent k. From our discussion of the individual terms it is apparent that at small values for k the increase in nuclear attraction energy dominates, such that the HF energy increases rapidly. At large distances, the kinetic energy and electron-electron interaction terms win, giving rise to convex curves for the plot E_{HF} versus k. The shape of these curves depends on the maximal principal quantum number n_{max} of the basis set. While a $(4,2,2)$ CS basis gives rise to the deepest minimum, for $(5,2,2)$ and $(6,2,2)$ the energy versus exponent curves become visibly flatter close to the optimal exponent (around $k = 2.8$). Since k only occurs in the radial part of the CS basis functions and larger values of n_{max} imply that the set of all radial functions R_{nl} becomes more complete, the value of k gets less important. Notice that not all parts of the energy versus exponent curves are equally dependent on n_{max}. As a result, the optimal exponent k_{opt} depends on n_{max} as well and larger basis sets give rise to smaller values for k_{opt}. This can be rationalized by taking the plots of the energy terms in Fig. 12 into account. The nuclear attraction energy is influenced by k most strongly and, additionally, it is (by magnitude) the largest contribution to the HF energy. In order to yield the minimal ground-state energy in a small basis, the dominating effect is therefore to minimize the nuclear attraction energy as much as possible. As a result, the optimal exponent k_{opt} takes comparatively large values. As the basis becomes larger, a balanced description of the complete physics becomes possible, such that the electron repulsion and kinetic effects are described better as well and thus smaller values for k_{opt} results. Moreover, the difference in magnitude of the energy terms rationalizes why choosing a CS exponent larger than k_{opt} will generally have a lesser influence on the obtained energy compared to choosing a too small exponent, which can be observed in Fig. 1 as well.

Due to the flat structure of the energy versus exponent curves close to the optimal exponent k_{opt}, it is not required at high accuracy. If a highly accurate treatment of a particular system is required, then increasing n_{max} has both a much larger effect and is computationally cheaper than finding the optimal exponent more accurately. A good estimate to k_{opt} for

a basis can be usually found by minimizing the HF energy with respect to k in a smaller basis and then use the obtained value for larger bases as well. Since such energy curves are convex and only scalar functions of a single parameter, this minimization can be performed effectively by a gradient-free optimization algorithm based on Brent's method [94]. Starting from a reasonable guess for k_{opt} convergence to the minimum is usually achieved in around 10 iterations, which requires a similar number of energy computations using the chosen quantum-chemical method and the chosen CS basis. An appropriate procedure for obtaining k_{opt} for HF is described in Ref. [95] and has been implemented in `molsturm` [49]. A selection of optimal exponents for the atoms of the second and third periods can be found in Tables SI-1 and SI-2 of the Supplemental Material [96].

C. Comparison of optimal Coulomb Sturmian exponents and the Slater exponents from Clementi and Raimondi [2]

Comparing the radial part of a Slater-type orbital [1,97]

$$R_n^{STO}(r) = \frac{(2\zeta)^{3/2}}{\sqrt{(2n)!}} (2\zeta r)^{n-1} \exp(-\zeta r) \qquad (16)$$

with the radial part of a CS function (4), one notices that the functional form is very similar, with the Slater exponent ζ and the CS exponent k occurring in related terms. Additionally, the procedure followed by Clementi and Raimondi [2] to obtain the Slater exponents $\zeta_{Clementi}$ is a variational minimization of the HF energy with respect to ζ, so the same approach we used to obtain k_{opt}. However, the notable difference between CS discretizations and STO bases is that all CS functions in a basis share the same k, whereas each function of an STO basis may employ a different ζ.

Instead of directly relating the values of k and $\zeta_{Clementi}$, we therefore plot k versus the occupation-weighted averaged of the $\zeta_{Clementi}$ values corresponding to the occupied orbitals of a respective atom (see Fig. 14). Over the full depicted range, the magnitude of k_{opt} and the average $\zeta_{Clementi}$ stays similar. Furthermore, except the sharp drop going from atom number 10 to 11 the trend of $\zeta_{Clementi}$ is more or less reproduced by k_{opt}. Notice, however, that the trend in both cases is not linear

as can be observed by comparing the data points to the fitted lines.

With respect to the drop between $Z = 10$ and 11, two possible causes are plausible. First, our calculations in the third period employs a larger CS basis set compared to the second period. This was done to provide extra basis functions for the description of the more electron-rich atoms. Recalling our discussion in Sec. III B related to Fig. 13, larger basis sets tend to lead to smaller values for k_{opt}. The observed drop in Fig. 14 is, however, much larger than any lowering caused by increasing the basis (see Tables SI-1 and SI-2 of the Supplemental Material [96]), such that additional effects need to be present. A second aspect to consider is the reduction of information, which is caused by taking the average of all $\zeta_{Clementi}$. For example, when changes in the physics of the electronic structure of the atom trigger relative adjustments of the exponents $\zeta_{Clementi}$, this is not captured by the average $\zeta_{Clementi}$. Especially when going to a new shell, i.e., when adding a new, more expanded orbital with only a single electron in it, the structure of the electron density undergoes large changes compared to the previous atom: the inner core electrons become more contracted while the atomic radius and thus the valence shell expands. The STO basis has more degrees of freedom in the form of multiple exponents to adapt to this, the CS basis has only one exponent to balance the effects. This potentially overemphasizes some trends, e.g., the compression of the core, compared to others, leading to deviations from the trend of the average $\zeta_{Clementi}$.

Nevertheless, the similarities in the trend between k_{opt} and the average $\zeta_{Clementi}$ allows for a physical interpretation of k_{opt}. Returning to the ideas of Slater [1], which were later picked up by Clementi and Raimondi [2], one can use the exponents $\zeta_{Clementi}$ to define, for each orbital, a shielding parameter σ, which indicates how much of the nuclear charge is screened away by all electrons closer to the core. The appropriate relationship is

$$\zeta_{Clementi} = \frac{Z - \sigma}{n^*},$$ (17)

where Z is the nuclear charge and n^* is a function of the principal quantum number (see Ref. [1]). $Z - \sigma$ is sometimes called the effective nuclear charge as well, giving it the interpretation as a measure for the remaining charge felt by an orbital. If we take k_{opt} to be related to the average $\zeta_{Clementi}$, we can think of k_{opt} as a measure for the average effective nuclear charge, which is felt by all electrons.

D. Selecting Coulomb Sturmian basis sets for Hartree-Fock calculations

As discussed, selecting CS basis sets for HF calculations boils down to selecting a reasonable exponent k together with values for n_{max} and l_{max} such that the basis does not get too large and the error in the discretization of the angular part as well as the radial part is balanced.

For cases where the RMSO$_l$ plots show a distinct drop at a particular angular moment, a suitable l_{max}, which fully captures the angular part, can be read off. What remains is to increase n_{max} until the radial part is sufficiently converged as well. For the examples considered in this work, $n_{max} = 10$ was

sufficient to reach a target accuracy of more than four digits in the HF energy, which equals a relative error of below 10^{-4}. For Li and Be, where $l_{max} = 0$ is sufficient, this translates to a $(10,0,0)$ basis consisting of only 10 CS basis functions. For the other atoms with a rapid-drop-type RMSO$_l$ plot, a $(10,1,1)$ basis would be required, which has 37 basis functions. In our investigation we obtained rapid-drop-type RMSO$_l$ plots for HF calculations on closed-shell atoms, on open-shell atoms with an S ground-state term, and for UHF calculations of any other open-shell atom if fractional occupation numbers were used. Given the arguments we outlined in Sec. II B, we expect these observations to extend to the other periods.

In case of a decreasing staircase pattern in the RMSO$_l$ plots one needs to find a balance: Restricting the CS basis set using smaller values of l_{max} implies a larger error in the angular discretization, but on the other hand gives rise to more manageable scaling of the basis-set size [see Eq. (11)]. This in turn implies that larger values for n_{max} can be used and thus that a more accurate radial discretization may be obtained. For example, for oxygen in a UHF calculation with integer occupation numbers at least $l_{max} = 3$ and $n_{max} = 10$ is required to reach five digits of accuracy compared to the CBS reference. This is a basis with the enormous number of 126 basis functions. For carbon, on the other hand, $l_{max} = 2$ is sufficient, such that a $(10,2,2)$ basis with 77 functions may be used. On the other hand, our discussion linked the occurrence of the decreasing staircase pattern in the RMSO$_l$ plots to a breaking of spherical symmetry in the UHF calculations. From this point of view one could argue to still use $l_{max} = 1$, however. This will effectively prevent the symmetry breaking by not providing any higher angular momentum in the basis. For UHF calculations of the second and third periods we therefore suggest to stick to $l_{max} = 1$. This approach, however, is not applicable to the higher periods since d functions are occupied as well. For performing accurate UHF calculations on open-shell systems in period 4 and onwards, either larger l_{max} values or techniques to prevent the breaking of spherical symmetry need to be used. Alternatively, one may still choose $l_{max} = 2$ and live with the uneven description of the spherical symmetry breaking in s, p, and d functions.

Compared to the influence of n_{max} and l_{max}, the value of the Coulomb Sturmian exponent k only plays a secondary role since it does not alter the convergence trends. Typically it is therefore sufficient to use a value which is reasonably close to the minimal-energy exponent k_{opt}. This can, for example, be achieved by reusing an optimal exponent from a smaller basis set, like the exponents provided in the Supplemental Material (Tables SI-1 and SI-2) [96].

IV. OUTLOOK

For judging the convergence properties of Coulomb Sturmians with respect to quantum-chemical simulations, Hartree-Fock is without any doubt only the first step. Nevertheless, already at the HF level this work only represents the first step. For example, restricted open-shell HF has not been considered at all so far and similarly we just stated empirical observations. A more mathematically motivated approach could allow to deduce rigorous error bounds and potentially allow to understand whether the observed sublinear convergence for

nitrogen and for the cases with a clear drop in $RMSO_l$ is a general feature, which would also be encountered for Be and Ne at large enough bases. Similarly, a more quantitative understanding on the deviation of the convergence rate with respect to choosing a CS exponent would be desirable.

With respect to capturing correlation effects, preliminary work [95] suggests that the leading-order effects can be captured by increasing l_{max} by 1, in agreement with the typical constructions followed for cGTO basis sets [5,6,57]. Our plan is to confirm this with a more detailed discussion in a subsequent publication. Given that a larger l_{max} bound will additionally increase the basis size beyond the HF level, primitive CS basis functions will probably not be sufficient any more. With respect to contracted CS basis sets, however, the challenge is to design construction schemes, which do not break the advantageous equivalence of the CS basis functions with the hyperspherical harmonics, which is required for an efficient evaluation of the CS ERI integrals [26,27]. For this reason, one should restrict the formation of contracted CS functions in a way that all primitives still share the same CS exponent k. The availability of contracted CS basis sets, constructed in such a way, would furthermore allow to use them in molecular calculations, which have now gotten into reach due to the recent advances in evaluating four-center electron-repulsion integrals using CS functions [25–28].

V. CONCLUSIONS

In recent, years exponential-type basis functions have shown to be promising alternatives for quantum-chemical simulations [9,10]. From this class of functions, Coulomb Sturmians (CS) are particularly appealing. These functions form a complete one-particle basis and furthermore their multicenter electron-repulsion integrals can be evaluated efficiently [25–28]. As a result, molecular problems could be treated with this basis in the future. Following along this prospect, this work provided a look at the construction of CS basis sets for quantum-chemical calculations. For this objective, a simple and physically motivated construction scheme for CS basis sets was suggested and its convergence properties with respect to atomic calculations at the Hartree-Fock (HF) level investigated. A brief outlook towards correlated and molecular calculations was provided as well.

In our construction, a CS basis set is formed by restricting the set of possible quantum number triples (n, l, m) using upper bounds n_{max}, l_{max}, and m_{max} on the principal, angular momentum, and magnetic quantum numbers, respectively. While the bound on n_{max} is required to achieve a finite basis size, the bounds l_{max} and m_{max} are optional, in which case only the usual restrictions between n, l, and m apply. The CS exponent k is common to all CS functions of the basis and is fixed as a fourth parameter of a basis.

With respect to the convergence properties k only effects the convergence rate, but not the observed convergence trends. Furthermore, for each choice of n_{max} and l_{max} an optimal, minimum-energy CS exponent k_{opt} can be found. Deviations from this value, however, become more and more unimportant as n_{max} gets larger. We have computed some optimal exponent values for the second and the third periods of the periodic

table, which can be found in the Supplemental Material [96]. From a plot of these k_{opt} exponents versus the atomic number, we identified similar trends to a plot of the average Slater exponents obtained by Clementi and Raimondi [2]. Based on these results, we suggested a physical interpretation of the optimal exponents k_{opt} as a measure for the average effective nuclear charge, which is felt by the electrons of an atom.

The basis parameters n_{max} and l_{max} were identified to independently influence the convergence of the CS discretization in the radial and angular coordinates, respectively. Additionally, these have a direct influence on the size of the CS basis, where introducing a restriction by $l_{max} \ll n_{max}$ reduces the scaling of the basis-set size from cubic in n_{max} to linear in n_{max}. A key aspect for constructing CS basis sets is therefore to fix l_{max} to a value causing both a sufficiently good angular discretization as well as the smallest basis sizes possible.

For this purpose, we introduced the root-mean-square occupied coefficient value per angular momentum l ($RMSO_l$). This quantity allows to measure the importance of a particular angular momentum quantum number l for describing a Hartree-Fock (HF) wave function. Considering the trend of $RMSO_l$ as l is increased thus either allows to directly select a value for l_{max} or help uncover unphysical effects such as the breaking of spherical symmetry in the UHF calculations on oxygen and carbon if integer occupation numbers are used. It should be noted that the construction of $RMSO_l$ is general and could be applied to other basis functions of the form radial part times spherical harmonics, for example, cGTO discretizations. Due to the completeness of the radial part of the Coulomb Sturmians, the observed $RMSO_l$ behavior for CS discretizations has general character, i.e., it should be reproduced by other basis function types as well.

With respect to the bound n_{max}, our investigations indicate that $n_{max} = 10$ is sufficient to give rise to 4 to 5 digits of accuracy in the HF energy for all our investigated cases. For lithium and beryllium, $l_{max} = 0$ showed to be suitable, whereas $l_{max} = 1$ should be chosen for the other atoms of the second and third periods. This value assumes, however, that a potential breaking of spherical symmetry in UHF should not be modeled or is prevented using, e.g., fractional occupation numbers. As indicated by our $RMSO_l$ plots, larger values for l_{max} are required otherwise, the precise value depending on the desired target accuracy.

In all cases considered, the convergence behavior of the proposed basis set construction could be interpreted based on physical arguments. This includes challenging cases like the symmetry breaking in some UHF calculations, where conversely the obtained $RMSO_l$ plots were used to gain an understanding of the unusual angular momentum requirements of such wave functions. For key basis parameters, such as l_{max} or the optimal exponent k_{opt}, physical interpretations were suggested. This emphasizes the ability of CS basis sets to capture the physics of HF wave functions and furthermore enables an intuitive approach to the construction of CS basis sets. In light of modern approaches for constructing cGTO basis sets, a thorough understanding of convergence properties of atoms at the HF level is the prerequisite for constructing contracted CS basis sets. This work enables such progress, bringing Coulomb Sturmian basis sets one step closer towards

applying them to correlated quantum-chemical methods and molecular systems.

[1] J. C. Slater, Phys. Rev. **36**, 57 (1930).

[2] E. Clementi and D. L. Raimondi, J. Chem. Phys. **38**, 2686 (1963).

[3] S. Huzinaga, J. Chem. Phys. **42**, 1293 (1965).

[4] W. J. Hehre, R. F. Stewart, and J. A. Pople, J. Chem. Phys. **51**, 2657 (1969).

[5] F. Jensen, WIREs Comput. Mol. Sci. **3**, 273 (2013).

[6] J. G. Hill, Int. J. Quantum Chem. **113**, 21 (2013).

[7] T. Kato, T. Am. Math. Soc. **70**, 195 (1951).

[8] T. Kato, Commun. Pure Appl. Math. **10**, 151 (1957).

[9] M. Güell, J. M. Luis, M. Solá, and M. Swart, J. Phys. Chem. A **112**, 6384 (2008).

[10] P. E. Hoggan, in *Self-Organization of Molecular Systems: From Molecules and Clusters to Nanotubes and Proteins*, edited by N. Russo, V. Y. Antonchenko, and E. S. Kryachko (Springer, Dordrecht, 2009), pp. 199–219.

[11] H. Feshbach, Ann. Phys. (NY) **5**, 357 (1958).

[12] H. Feshbach, Ann. Phys. (NY) **19**, 287 (1962).

[13] U. V. Riss and H.-D. Meyer, J. Phys. B: At. Mol. Phys. **26**, 4503 (1993).

[14] R. Santra and L. S. Cederbaum, Phys. Rep. **368**, 1 (2002).

[15] F. Harris and H. Michels, Adv. Chem. Phys. **13**, 205 (1967).

[16] E. Steinborn, in *Methods in Computational Molecular Physics*, edited by G. Dierksen and S. Wilson (Reidel, Dordrecht, 1983)

[17] E. Weniger and E. Steinborn, J. Chem. Phys. **78**, 6121 (1983).

[18] *International Conference on ETO Multicenter Integrals*, edited by C. Weatherford and H. Jones (Reidel, Dordrecht, 1982).

[19] H. Shull and P.-O. Löwdin, J. Chem. Phys. **30**, 617 (1959).

[20] M. Rotenberg, Ann. Phys. (NY) **19**, 262 (1962).

[21] M. Rotenberg, in *Advances in Atomic and Molecular Physics*, Vol. 6, edited by D. Bates and I. Esterrnan (Academic, New York, 1970), pp. 233–268.

[22] A. Vincenzo, C. Andrea, and C. Simonetta, Int. J. Quantum Chem. **92**, 99 (2003).

[23] C. Coletti, D. Calderini, and V. Aquilanti, Adv. Quantum Chem. **67**, 73 (2013).

[24] D. Calderini, S. Cavalli, C. Coletti, G. Grossi, and V. Aquilanti, J. Chem. Sci. **124**, 187 (2012).

[25] J. S. Avery and J. E. Avery, Mol. Phys. **110**, 1593 (2012).

[26] J. E. Avery, Adv. Quantum Chem. **67**, 129 (2013).

[27] J. E. Avery and J. S. Avery, Adv. Quantum Chem. **70**, 265 (2015).

[28] J. E. Avery and J. S. Avery, Adv. Quantum Chem. **76**, 133 (2017).

[29] J. E. Avery and J. S. Avery, *Generalized Sturmians and Atomic Spectra* (World Scientific, Singapore, 2006).

[30] V. Aquilanti, S. Cavalli, C. Coletti, and G. Grossi, Chem. Phys. **209**, 405 (1996).

[31] V. Aquilanti, S. Cavalli, and C. Coletti, Chem. Phys. **214**, 1 (1997).

[32] V. Aquilanti, S. Cavalli, and C. Coletti, Phys. Rev. Lett. **80**, 3209 (1998).

[33] J. S. Avery and J. E. Avery, Adv. Quantum Chem. **43**, 185 (2003).

[34] J. S. Avery, J. E. Avery, V. Aquilanti, and A. Caligiana, Adv. Quantum Chem. **47**, 157 (2004).

[35] J. E. Avery and J. S. Avery, J. Math. Chem. **46**, 164 (2009).

[36] D. Calderini, C. Coletti, G. Grossi, and V. Aquilanti, in *Computational Science and Its Applications–ICCSA 2013*, edited by B. Murgante, S. Misra, M. Carlini, C. M. Torre, H.-Q. Nguyen, D. Taniar, B. O. Apduhan, and O. Gervasi (Springer, Berlin, 2013), pp. 32–45.

[37] A. Abdouraman, A. Frapiccini, A. Hamido, F. Mota-Furtado, P. O'Mahony, D. Mitnik, G. Gasaneo, and B. Piraux, J. Phys. B: At., Mol. Opt. Phys. **49**, 235005 (2016).

[38] J. S. Avery, *Hyperspherical Harmonics: Applications in Quantum Theory* (Springer, Berlin, 1989).

[39] V. Aquilanti and S. Cavalli, in *Few-Body Problems in Physics*, edited by C. Ciofi degli Atti, E. Pace, G. Salmè, and S. Simula (Springer, Vienna, 1992), pp. 573–580.

[40] V. Aquilanti, A. Lombardi, and R. G. Littlejohn, Theor. Chem. Acc. **111**, 400 (2004).

[41] J. E. Avery and J. S. Avery, *Hyperspherical Harmonics and Their Physical Applications* (World Scientific, Singapore, 2018).

[42] T. K. Das, *Hyperspherical Harmonics Expansion Techniques* (Springer, Berlin, 2016).

[43] J. M. Randazzo, L. U. Ancarani, G. Gasaneo, A. L. Frapiccini, and F. D. Colavecchia, Phys. Rev. A **81**, 042520 (2010).

[44] D. M. Mitnik, F. D. Colavecchia, G. Gasaneo, and J. M. Randazzo, Comput. Phys. Commun. **182**, 1145 (2011).

[45] M. J. Ambrosio, F. D. Colavecchia, D. M. Mitnik, G. Gasaneo, and L. U. Ancarani, J. Phys.: Conf. Ser. **601**, 012004 (2015).

[46] C. M. Granados-Castro, L. U. Ancarani, G. Gasaneo, and D. M. Mitnik, J. Phys.: Conf. Ser. **601**, 012009 (2015).

[47] J. M. Randazzo, D. Mitnik, G. Gasaneo, L. U. Ancarani, and F. D. Colavecchia, Eur. Phys. J. D **69**, 189 (2015).

[48] C. M. Granados-Castro, L. U. Ancarani, G. Gasaneo, and D. M. Mitnik, Adv. Quantum Chem. **73**, 3 (2016).

[49] M. F. Herbst, A. Dreuw, and J. E. Avery, J. Chem. Phys. **149**, 84106 (2018).

[50] B. Klahn and W. A. Bingel, Theor. Chim. Acta **44**, 9 (1977).

[51] B. Klahn and W. A. Bingel, Theor. Chim. Acta **44**, 27 (1977).

[52] J. E. Avery, The generalised Sturmian method, Master's thesis, University of Copenhagen, 2008.

[53] G. Teschl, *Mathematical Methods in Quantum Mechanics: With Applications to Schrödinger Operators*, 2nd ed. (American Mathematical Society, Providence, RI, 2014).

[54] M. M. Francl, W. J. Pietro, W. J. Hehre, J. S. Binkley, M. S. Gordon, D. J. DeFrees, and J. A. Pople, J. Chem. Phys. **77**, 3654 (1982).

[55] R. Krishnan, J. S. Binkley, R. Seeger, and J. A. Pople, J. Chem. Phys. **72**, 650 (1980).

[56] P. C. Hariharan and J. A. Pople, Theor. Chim. Acta **28**, 213 (1973).

[57] L. Kong, F. Bischoff, and E. Valeev, Chem. Rev. **112**, 75 (2012).

[58] T. H. Dunning, J. Chem. Phys. **90**, 1007 (1989).

[59] F. Jensen, J. Chem. Phys. **136**, 114107 (2012).

[60] D. B. Cook, Theor. Chim. Acta **58**, 155 (1981).

[61] H. Fukutome, Int. J. Quantum Chem. **20**, 955 (1981).

[62] D. B. Cook, Mol. Phys. **53**, 631 (1984).

[63] R. McWeeny and B. Sutcliffe, Comput. Phys. Rep. **2**, 219 (1985).

[64] C. C. J. Roothaan, Rev. Mod. Phys. **23**, 69 (1951).

[65] J. A. Pople and R. K. Nesbet, J. Chem. Phys. **22**, 571 (1954).

[66] A. Szabo and N. S. Ostlund, *Modern Quantum Chemistry*, 1st ed. (Dover, New York, 1996).

[67] B. Sutcliffe, E. Cancès, M. Caffarel, R. Assaraf, G. Turinici, I. Catto, P.-L. Lions, C. Le Bris, O. Bokanowski, B. Grébert, N. J. Mauser, X. Blanc, M. Defranceschi, V. Louis-Achille, B. Mennucci, J. Dolbeault, M. J. Esteban, E. Séré, T. Saue, and H. J. A. Jensen, in *Mathematical Models and Methods for Ab Initio Quantum Chemistry*, edited by M. Defranceschi and C. Le Bris, Lecture Notes in Chemistry, Vol. 74 (Springer, Berlin, 2000).

[68] E. Cancès and C. Le Bris, Int. J. Quantum Chem. **79**, 82 (2000).

[69] E. Cancès and C. Le Bris, ESAIM: M2AN **34**, 749 (2000).

[70] H. C. Longuet-Higgins and J. A. Pople, Proc. Phys. Soc. London, A **68**, 591 (1955).

[71] M. J. S. Dewar, J. A. Hashmall, and C. G. Venier, J. Am. Chem. Soc. **90**, 1953 (1968).

[72] J. C. Slater, J. B. Mann, T. M. Wilson, and J. H. Wood, Phys. Rev. **184**, 672 (1969).

[73] M. J. S. Dewar and N. Trinajstic, J. Chem. Soc. D, 646b (1970).

[74] F. Ellison and F. Matheu, Chem. Phys. Lett. **10**, 322 (1971).

[75] P. Čársky and R. Zahradník, Theor. Chim. Acta **26**, 171 (1972).

[76] C. C. J. Roothaan, Rev. Mod. Phys. **32**, 179 (1960).

[77] V. Bach, E. H. Lieb, M. Loss, and J. P. Solovej, Phys. Rev. Lett. **72**, 2981 (1994).

[78] J. E. Avery and M. F. Herbst, https://molsturm.org/sturmint.

[79] M. F. Herbst and T. Wackenhut, mfherbst/SelfConsistentField.jl v0.0.0, doi: 10.5281/zenodo.1481714.

[80] G. van Rossum, Python tutorial, Technical Report No. CS-R9526 (Centrum voor Wiskunde en Informatica (CWI), Amsterdam, 1995).

[81] J. Bezanson, A. Edelman, S. Karpinski, and V. Shah, SIAM Rev. **59**, 65 (2017).

[82] S. van der Walt, S. C. Colbert, and G. Varoquaux, Comput. Sci. Eng. **13**, 22 (2011).

[83] E. Jones, T. Oliphant, P. Peterson *et al.*, SciPy: Open source scientific tools for Python.

[84] W. McKinney, J. Reback *et al.*, pandas: Python data analysis library.

[85] J. D. Hunter, Comput. Sci. Eng. **9**, 90 (2007).

[86] D. E. Woon and T. H. Dunning, J. Chem. Phys. **98**, 1358 (1993).

[87] N. H. Morgon, R. Custodio, and J. Mohallem, J. Mol. Struct.: THEOCHEM **394**, 95 (1997).

[88] A. K. Wilson, T. van Mourik, and T. H. Dunning, J. Mol. Struct.: THEOCHEM **388**, 339 (1996).

[89] T. Van Mourik and T. H. Dunning, Int. J. Quantum Chem. **76**, 205 (2000).

[90] B. P. Prascher, D. E. Woon, K. A. Peterson, T. H. Dunning, and A. K. Wilson, Theor. Chem. Acc. **128**, 69 (2011).

[91] F. Jensen, Theor. Chem. Acc. **113**, 267 (2005).

[92] B. Helffer, *Spectral Theory and its Applications* (Cambridge University Press, Cambridge, UK, 2013).

[93] M. Bachmayr, H. Chen, and R. Schneider, Numer. Math. **128**, 137 (2014).

[94] R. P. Brent, *Algorithms for Minimization without Derivatives* (Prentice-Hall, Englewood Cliffs, NJ, 1972), Chaps. 3 and 4.

[95] M. F. Herbst, Development of a modular quantum-chemistry framework for the investigation of novel basis functions, Ph.D. thesis, Ruprecht-Karls-Universität Heidelberg, 2018, https://michael-herbst.com/publications/2018.05_phd_corrected.pdf

[96] See Supplemental Material at http://link.aps.org/supplemental/10.1103/PhysRevA.99.012512 for a selection of optimal Coulomb Sturmian exponents for the atoms of the second and third periods.

[97] T. Helgaker, J. Olsen, and P. Jorgensen, *Molecular Electronic-Structure Theory*, 1st ed. (Wiley, Chichester, 2013).